

## Elastic and inelastic scattering of $^{40}\text{Ar}$ from $^{208}\text{Pb}$ at 236 MeV

U. Arlt, R. Bass, V. Hartmann, R. Renfordt, and K. Sapotta

*Institut für Kernphysik der Universität Frankfurt, D-6000 Frankfurt am Main, Germany*

P. Fröbrich

*Hahn-Meitner-Institut and Freie Universität Berlin, D-1000 Berlin, West Germany*

W. Schäfer\*

*Gesellschaft für Schwerionenforschung, D-6100 Darmstadt, Germany*

(Received 13 May 1980)

The scattering of  $^{40}\text{Ar}$  from  $^{208}\text{Pb}$  at 236 MeV has been measured with sufficient energy resolution to separate elastic from inelastic scattering. The results demonstrate the importance of long-range absorption due to strong Coulomb interaction and are well reproduced by appropriate theoretical calculations.

NUCLEAR REACTIONS  $^{208}\text{Pb}(^{40}\text{Ar}, ^{40}\text{Ar})$ ,  $^{208}\text{Pb}(^{40}\text{Ar}, ^{40}\text{Ar}')$ ,  $E = 236$  MeV, measured  $\sigma(\theta)$ , optical model analysis with dynamic polarization potential, semiclassical analysis of inelastic scattering. Enriched target.

Elastic scattering of heavy ions above the Coulomb barrier generally exhibits diffraction-like angular distributions of Fraunhofer or Fresnel type<sup>1</sup> which arise from an absorptive nuclear interaction of well-defined, short range. A qualitatively different behavior is expected, however, for very heavy scattering systems and not too high bombarding energies, where the long-range Coulomb interaction is sufficiently strong to induce large absorption probabilities at distances well beyond the nuclear strong absorption radius.<sup>2-5</sup> Under these circumstances the differential elastic cross section should fall significantly below the Rutherford value at angles much smaller than the grazing angle. This phenomenon has indeed been observed for several scattering systems involving comparatively light projectiles ( $^{16}\text{O}$ ,  $^{20}\text{Ne}$ ) and heavy target nuclei ( $^{184}\text{W}$ ,  $^{208}\text{Pb}$ ), where low-lying collective states of either target or projectile are strongly excited by Coulomb excitation.<sup>6,7</sup>

With still heavier projectiles ( $A \geq 40$ ) Coulomb-dominated absorption is expected even in the absence of strong collective enhancements, and should therefore represent a rather general phenomenon. Nevertheless, previously published data for "elastic scattering" of  $^{40}\text{Ar}$  and heavier projectiles from heavy targets do not show the effect, but rather exhibit a conventional Fresnel pattern.<sup>8-10</sup> This can be explained by the limited energy resolution of these earlier studies, which prevented the separation of the elastic group from low-lying inelastic groups at total kinetic energies of several hundreds of MeV. Evidently the inclusion of certain inelastic groups in the "quasi-elastic" angular distribution restores—at least

qualitatively—the Fresnel pattern which is typical for purely nuclear absorption.

It might be argued that there is no point in resolving elastic scattering from strongly Coulomb-excited inelastic transitions, as long as one is interested only in the nuclear interactions. The latter one might hope to deduce from an optical or diffraction model analysis of the combined quasielastic angular distribution. However, in general it is not clear *a priori* which inelastic components should be included and to what extent nuclear effects are mixed in with Coulomb excitation. Thus the parameters extracted from the model analysis would be of limited significance.

Therefore, in the present study we have made an effort to resolve elastic and inelastic scattering for a heavy system,  $^{40}\text{Ar} + ^{208}\text{Pb}$ , at an energy about 20% above the interaction barrier. The purpose of this work was, firstly, to demonstrate the importance of Coulomb-induced absorption for elastic scattering and to test the validity of a recent approximate treatment of this effect, in which the coupling to inelastic channels via Coulomb excitation is simulated by the use of a "dynamic polarization potential."<sup>2</sup> Secondly, it was hoped to obtain information on the sensitivity of the elastic and inelastic cross sections to the nuclear part of the nucleus-nucleus interaction, and on the presence or absence of Coulomb-nuclear interference effects.

The experiment was performed at the UNILAC accelerator of Gesellschaft für Schwerionenforschung (GSI), Darmstadt, using a 5.9 MeV/u (236 MeV)  $^{40}\text{Ar}$  beam and highly enriched (98.7%) metallic  $^{208}\text{Pb}$  targets of nominal thickness 100

$\mu\text{g}/\text{cm}^2$ , evaporated onto approximately  $20 \mu\text{g}/\text{cm}^2$  carbon backings. The scattered particles were detected at laboratory angles between  $35^\circ$  and  $72^\circ$  ( $\theta_{\text{c.m.}} = 41.3\text{--}82.5^\circ$ ) with a high-resolution time-of-flight spectrometer which incorporates a flight path of 5 m and magnetic quadrupole focusing.<sup>11</sup> The latter feature results in a solid angle of 0.5 msr with an angular resolution of about  $0.1^\circ$ . The instrument permits the simultaneous measurement of time-of-flight, energy loss (in a gas-filled ionization chamber) and residual energy (deposited in an array of surface barrier detectors). These observables were recorded event by event on magnetic tape and used later in the off-line construction of time-of-flight (energy) spectra for selected combinations  $A, Z$  with complete resolution of isotopes.

In order to resolve elastic scattering from inelastic scattering to the lowest  $2^+$  state in  $^{40}\text{Ar}$  at 1.46 MeV an energy resolution of less than 0.5% was required at our bombarding energy. While our instrumental energy resolution, as derived from the time-of-flight measurement, was significantly better than this value ( $\leq 0.3\%$ ), it was found that in practice the overall energy resolution was limited by the spread in beam energy and by target inhomogeneities produced by the beam. Figure 1 shows time-of-flight spectra of scattered  $^{40}\text{Ar}$  particles as observed at laboratory angles of  $50^\circ$  and  $70^\circ$ , respectively. Although the elastic and inelastic groups are not clearly separated, it was possible to extract the intensities corresponding to  $Q=0$  and  $Q=-1.46$  MeV by fitting Gaussian line shapes centered at the expected positions. This procedure should be quite accurate for the

elastic group, but introduces some uncertainty for the intensities of the 1.46 MeV transition. It is interesting to note that unresolved states above 2 MeV total excitation energy are produced significantly at  $70^\circ$ , but are practically absent at  $50^\circ$  (or below).

Measurements were taken at  $5^\circ$  intervals between  $35^\circ$  and  $70^\circ$ , with additional points at  $68^\circ$  and  $72^\circ$  in the laboratory system. Relative normalization of the data was obtained by referring to two monitor counters which were positioned at fixed angles of  $16^\circ$  and  $19^\circ$  with respect to the beam direction. Finally, the absolute scale of the cross sections was determined by normalizing the sum of the elastic and inelastic cross sections to the Rutherford value at the smallest measured angle of  $35^\circ$ . The differential cross sections derived in this manner for the  $0^+$  and  $2^+$  final states—divided in each case by the Rutherford cross section—are shown in Fig. 2. The effect of Coulomb excitation on the elastic scattering cross section is clearly evident.

The following theoretical analysis of the experimental data has been performed. The elastic scattering cross section was calculated using the electrodynamic dynamical polarization potential of Ref. 2 in addition to a nuclear Woods-Saxon potential. Besides the monopole-quadrupole interaction, we have also included the monopole-octupole interaction, because it turns out to have a non-negligible effect on the elastic angular distribution. The monopole-quadrupole contribution to the imaginary polarization potential was taken from Ref. 2, while for the monopole-octupole contribution we find ( $R_c$  = Coulomb radius)

$$\text{Im}U_p^{\lambda=3}(R) = \begin{cases} -\left[1 - \frac{1}{3}\left(\frac{R_c}{R}\right)^2 - \frac{2}{33}\left(\frac{R_c}{R}\right)^4\right] \frac{K_c(R)}{R^7} W_p^{\lambda=3} & \text{for } R \geq R_c, \\ -\frac{20}{33}\left(\frac{R}{R_c}\right)^6 \frac{K_c(R_c)}{R_c^7} W_p^{\lambda=3} & \text{for } R < R_c, \end{cases} \quad (1)$$

where the interaction strength is

$$W_p^{\lambda=3} = 0.00684 \frac{\mu Z^2 B(E3, 0 \rightarrow 3)}{k} g_{\lambda=3}(\xi), \quad (2)$$

and  $\mu$  is the reduced mass in atomic mass units,  $k$  the momentum (in  $\text{fm}^{-1}$ ),  $Z$  the monopole strength, and  $B(E3)$  is in ( $e^2 \text{fm}^6$ ). The quantity  $K_c(R) = [1 - Z_1 Z_2 e^2 / RE_{\text{c.m.}}]^{-1/2}$  is a correction factor due to the local momentum approximation and  $g_{\lambda=3}(\xi)$  is an adiabaticity correction factor well known from Coulomb excitation theory. For further details of the notation see Ref. 2.

The calculations of the elastic cross section have been performed with a quantal optical model code and alternatively with the semiclassical method of

using complex trajectories developed in Ref. 12. Both procedures give the same result. Because the polarization potential is of long range, about 700 partial waves have to be used. This corresponds to terminating the calculation at an  $l$  value where  $|S_l| - 1 < 10^{-4}$  ( $S_l$  is the elastic scattering matrix). The calculations show that the observed deviation from the Fresnel pattern in the elastic angular distribution is mainly due to the Coulomb excitation of the first  $2^+$  state [ $E = 1.46$  MeV,  $B(E2) = 382 e^2 \text{fm}^4$ ] in  $^{40}\text{Ar}$  (see curve 2 in Fig. 2). Adding the contribution of the  $3^-$  state [ $E = 2.61$  MeV,  $B(E3) = 665.10^3 e^2 \text{fm}^6$ ] in  $^{208}\text{Pb}$  gives only half of the remaining difference to the experimental data. Including furthermore the states with  $I^\pi = 2^+$

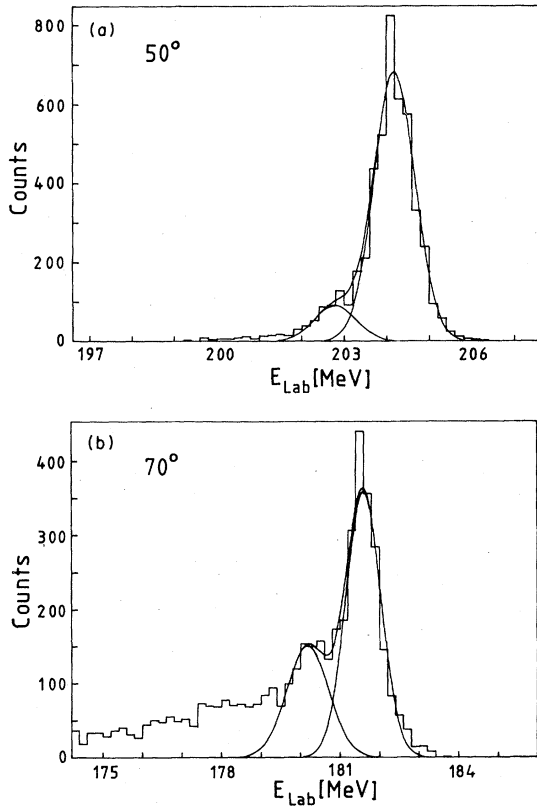


FIG. 1. Time-of-flight spectra (calibrated in terms of laboratory energies) of scattered  $^{40}\text{Ar}$  nuclei at laboratory angles of  $50^\circ$  ( $\theta_{\text{c.m.}} = 58.5^\circ$ , upper part) and  $70^\circ$  ( $\theta_{\text{c.m.}} = 80.4^\circ$ , lower part). Gaussian peak shapes are fitted to the elastic group and the inelastic group corresponding to excitation of the 1.46 MeV level ( $2^+$ ) in  $^{40}\text{Ar}$ .

$[E = 2.52 \text{ MeV}, B(E2) = 63.2 e^2 \text{ fm}^4]$ ,  $2^+[E = 3.21 \text{ MeV}, B(E2) = 29.3 e^2 \text{ fm}^4]$ ,  $3^-[E = 3.68 \text{ MeV}, B(E3) = 8750 e^2 \text{ fm}^6]$  in  $^{40}\text{Ar}$  and  $2^+[E = 4.07 \text{ MeV}, B(E2) = 3000 e^2 \text{ fm}^4]$  in  $^{208}\text{Pb}$  gives a very satisfactory agreement with experiment (curve 3 in Fig. 2).

The nuclear part of the optical model potential was taken from Ref. 7 where a coupled channels analysis of  $^{20}\text{Ne} + ^{208}\text{Pb}$  scattering was performed ( $V = 21.5 \text{ MeV}$ ,  $r_0 = 1.34 \text{ fm}$ ,  $a = 0.49 \text{ fm}$ ;  $W = 7.0 \text{ MeV}$ ,  $r'_0 = 1.43 \text{ fm}$ ,  $a' = 0.30 \text{ fm}$ ). This potential accounts well for the present results, whereas no acceptable fit was obtained with the potentials given in Ref. 8, which are based on an analysis of incompletely resolved scattering data for several heavy systems.

Because a full quantal coupled channel calculation is not feasible for a system as heavy as  $^{40}\text{Ar}$  on  $^{208}\text{Pb}$  one has to calculate the angular distribution for the  $2^+$  state in  $^{40}\text{Ar}$  in an approximate way. We have obtained the inelastic cross sections by calculating the Coulomb excitation probabilities

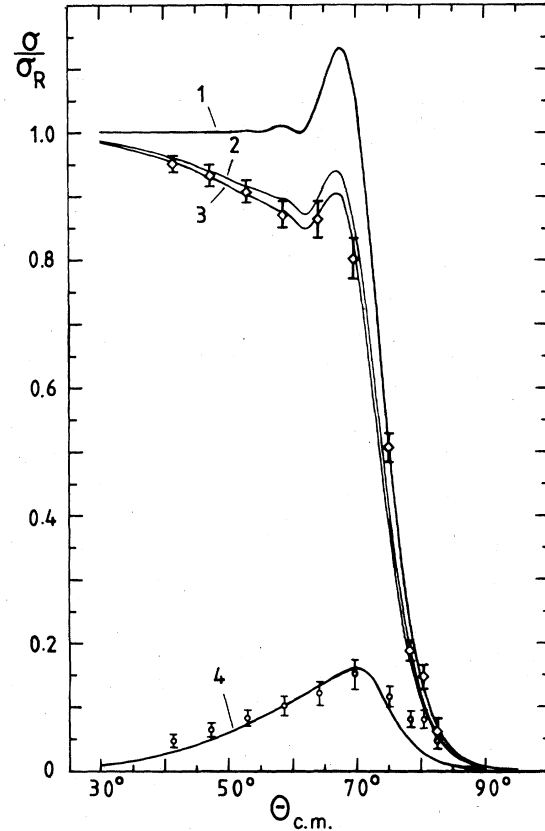


FIG. 2. Differential cross sections divided by the corresponding Rutherford values for elastic and inelastic scattering of  $^{40}\text{Ar}$  from  $^{208}\text{Pb}$ . Curve 1 is the elastic cross section calculated with a standard optical model potential from Ref. 7. Curves 2 and 3 are elastic cross sections calculated with inclusion of the dynamic polarization potential from Ref. 2 as explained in the text, while curve 4 is the inelastic ( $2^+$ ,  $Q = -1.46 \text{ MeV}$ ) cross section derived from Eq. (3). The experimental data are shown as open diamonds (elastic) and open circles (inelastic).

$P_I(\theta)$  with the semiclassical de Boer-Winther code,<sup>13</sup> and multiplying them by the elastic cross section due to the nuclear potential only, as derived from the standard optical model (OM) without polarization terms:

$$\left(\frac{d\sigma}{d\Omega}\right)_I = P_I(\theta) \left(\frac{d\sigma}{d\Omega}\right)_{\text{OM}}. \quad (3)$$

This approach gives not only very good agreement with the inelastic ( $I=2$ ) data (see Fig. 2) but also with the elastic angular distribution ( $I=0$ ).

In conclusion we can say that the present results are reproduced quantitatively in the elastic case by applying the theory of Ref. 2 to projectile and target excitations, and in the inelastic case by a factorization of the cross section into a nuclear

part and an electromagnetic excitation probability. The success of these simple models and the absence of appreciable Coulomb-nuclear interference effects show that the scattering is dominated beyond the strong absorption distance by the Coulomb interaction and at smaller distances by complicated nuclear rearrangements, while the nuclear excitation of low-lying collective states is comparatively unimportant. Similarly we see no evidence for excitation of giant multipole resonances at higher excitation energies. This situation should be typical for heavy scattering systems, such as the present one, and bombarding

energies not far above the Coulomb barrier.

The collaboration of J. V. Czarnecki and R. Zitzmann during the early stages of the present work and the support of our colleagues at the Gesellschaft für Schwerionenforschung (GSI), in particular R. Bock and F. Pühlhofer, are gratefully acknowledged. Thanks are due also to the technical staff of the GSI for providing the  $^{40}\text{Ar}$  beam and many other services. The work was supported financially by GSI and the Bundesministerium für Forschung und Technologie of the Federal Republic of Germany.

---

\*Present address: DEGUSSA, D-6450 Hanau, Germany.

<sup>1</sup>W. E. Frahn, Phys. Rev. Lett. **26**, 568 (1971).

<sup>2</sup>W. G. Love, T. Terasawa, and G. R. Satchler, Phys. Rev. Lett. **39**, 6 (1977); Nucl. Phys. **A291**, 183 (1977).

<sup>3</sup>A. J. Baltz, S. K. Kauffmann, N. K. Glendenning, and K. Pruess, Phys. Rev. Lett. **40**, 20 (1978); Nucl. Phys. **A327**, 221 (1979).

<sup>4</sup>W. E. Frahn, Nucl. Phys. **A302**, 301 (1978).

<sup>5</sup>P. Fröbrich, R. Lipperheide, and H. Fiedeldey, Phys. Rev. Lett. **43**, 1147 (1979).

<sup>6</sup>C. E. Thorn *et al.*, Phys. Rev. Lett. **38**, 384 (1977).

<sup>7</sup>E. E. Gross *et al.*, Phys. Rev. C **17**, 1665 (1978).

<sup>8</sup>J. R. Birkelund *et al.*, Phys. Rev. C **13**, 133 (1976).

<sup>9</sup>R. Vandenbosch *et al.*, Phys. Rev. C **13**, 1893 (1976).

<sup>10</sup>Y. T. Oganessian, Y. E. Penionzhkevich, V. I. Man'ko, and V. N. Polyansky, Nucl. Phys. **A303**, 259 (1978).

<sup>11</sup>R. Bass, J. v. Czarnecki, and R. Zitzmann, Nucl. Instrum. Methods **130**, 125 (1975).

<sup>12</sup>P. Fröbrich and P. Kaufmann, Nucl. Phys. **A307**, 297 (1978).

<sup>13</sup>J. de Boer and Aa. Winther, in *Coulomb Excitation*, edited by K. Alder and Aa. Winther (Academic, New York, 1966).